Food Hydrocolloids 95 (2019) 551–561

Contents lists available at ScienceDirect

Food Hydrocolloids

journal homepage: www.elsevier.com/locate/foodhyd

Fast preparation of rhamnogalacturonan I enriched low molecular weight pectic polysaccharide by ultrasonically accelerated metal-free Fenton reaction

Junhui Li[a], Shan Li[a], Yangfan Zheng[a], Hua Zhang[a], Jianle Chen[a], Lufeng Yan[a], Tian Ding[a], Robert J. Linhardt[b], Caroline Orfila[c], Donghong Liu[a], Xingqian Ye[a], Shiguo Chen[a,*]

[a] Zhejiang Key Laboratory for Agro-Food Processing, Department of Food Science and Nutrition, Fuli Institute of Food Science, Zhejiang University, Hangzhou 310058, China

[b] Center for Biotechnology & Interdisciplinary Studies, Department of Chemistry & Chemical Biology, Rensselaer Polytechnic Institute, Biotechnology Center 4005, Troy, NY 12180, USA

[c] School of Food Science and Nutrition, University of Leeds, Leeds LS2 9JT, UK

ARTICLE INFO

Keywords:
Citrus canning water
Pectic polysaccharide
Non-metal Fenton chemistry
Ultrafast green degradation
Antitumor activity

ABSTRACT

The recovery of pectic polysaccharides with high rhamnogalacturonan I (RG-I) branches from citrus canning processing water was achieved in a previous study aimed at reducing chemical oxygen demand and benefiting both process economics and the environment. However, the large molecular size and poor *in vivo* bioavailability of these polysaccharides limit the application of these pectic polysaccharides in functional foods. We report the development of an ultrafast and green approach to depolymerize pectic polysaccharides using an ultrasound-accelerated metal-free Fenton chemistry, relying on H_2O_2/ascorbic acid. The results show that ultrasound enhances the efficiency of H_2O_2/ascorbic acid system to degrade pectin into 7.9 kDa pectic fragments within 30 min through both chemical effects (increasing the amount of hydroxyl radicals and lowering activation energy of H_2O_2 decomposition) and mechanical effects (disaggregating polysaccharide clusters). The backbones of the resulting fragments mainly correspond to RG-I patterns (molar ratio galacturonic acid (GalA): rhamnose (Rha) ~ 1.06:1) with a high degree of rhamnose branching. Free radicals preferentially act on the GalA backbone in the HG region and maintain the RG-I region. Antitumor activities, assessed using human breast cancer cells (MCF-7), suggest that the resulting fragments significantly inhibit cancer cell growth and that activity increases with decreasing molecular weight. The resulting ultralow molecular weight pectic fragments have potential application for the development of functional foods and antitumor drugs.

1. Introduction

Canned citrus segments occupy an important sector of the world's fruit production, with an annual trade value of nearly $900 million (source: UN Comtrade). As the largest citrus planting and harvesting country in the world, China accounts for near 70% canned citrus segments on the international market (Wu et al., 2016). However, the industry produces about one million pounds of solid and liquid waste (principally polysaccharides) with high chemical oxygen demand (COD) (~10 000 mg/L) every year, representing both an economic and an environmental challenge (Chen et al., 2017). The organic substances present in the processing water mainly consist of pectic polysaccharides (PPs) (Chen et al., 2017) and these polysaccharides have potential use in food industry as thickeners and gelling agents.

In our previous study, we recovered PPs from basic water during the segment membrane removal process, taking place in citrus canning factories. These PPs were dominated by rhamnogalacturonan I regions with almost no esterification (Chen et al., 2017). RG-I enriched PPs, in dietary sources, are known to demonstrate a broad range of pharmacologic properties, such as antitumor (Zhi et al., 2017), prebiotic (Karboune & Khodaei, 2016), and immunomodulatory activities (Dikeman & Fahey, 2006). Despite multiple biomedical uses, these PPs have high molecular weights and, thus, show poor solubility and marginal bioavailability (Moreno & Sanz, 2014). Recent research has demonstrated that low-molecular-weight pectin polysaccharides (LMPs) have improved bioavailability (Kapoor & Dharmesh, 2017), greater prebiotic potential (Belén Gómez, Yáñez, Schols, & Alonso, 2016) and higher immune-modulating (Matsumoto, Guo, Ikejima, &

* Corresponding author. College of Biosystem Engineering and Food Science, Zhejiang University, Hangzhou 310029, China.
E-mail address: chenshiguo210@163.com (S. Chen).

https://doi.org/10.1016/j.foodhyd.2018.05.025
Received 2 March 2018; Received in revised form 11 May 2018; Accepted 12 May 2018
Available online 15 May 2018
0268-005X/

Yamada, 2003; Matsumoto et al., 2008; Shin, Kiyohara, Matsumoto, & Yamada, 1997), anti-ulcer and anti-inflammatory activities. Therefore, the preparation of LMPs is currently of great interest. However, to the best of our knowledge, the preparation of LMPs from citrus canning processing water has not been reported.

Controlled chemical depolymerization processes, mainly relying on acid or enzymatic treatment (Khodaei & Karboune, 2016; Khotimchenko, Kovalev, Kolenchenko, & Khotimchenko, 2012; Leclere, Cutsem, & Michiels, 2013; Hao et al., 2013) and physical treatments, such as ultrasound (Zhang et al., 2013), heat (Leclere et al., 2013; Ramos-Aguilar et al., 2015), high pressure microfluidization (Chen et al., 2013) and gamma-irradiation (Dogan, Kayacier, & Ic, 2007) have been used to prepare LMPs. The conditions for acid-catalyzed hydrolysis are usually fairly drastic, leading to the cleavage of different glycosidic linkages with low selectivity, and results in a variety of different LMP preparations (Garna, Mabon, Wathelet, & Paquot, 2004). Enzymatic hydrolysis of pectin is more selective, but requires the use of different types of enzymes, increasing the costs of the depolymerization process. In addition, during hydrolysis, potential microbial contamination of LMP preparations can result in decreased yields and lead to the formation of unwanted byproducts, further limiting its broad industrial application (Grohmann, Cameron, & Buslig, 1995). Among all the physical treatments reported, ultrasound is considered one of the most effective of the “green” techniques (Ma et al., 2016) used to depolymerize diverse forms of polysaccharides (Zhang et al., 2013). However, the reduction of polysaccharide molecular weight using ultrasound is typically limited to 20 kDa due to the attenuation of energy transmission under prolonged or high-intensity ultrasonic fields (Sun, Ma, Ye, Kakuda, & Meng, 2010).

A combination of a Fenton process with ultrasound can significantly improve degradation efficiency, as demonstrated in the pectin depolymerization process (Zhi et al., 2017). However, strictly acidic conditions (pH $<$ 4) are required in practical applications (Garrido-Ramirez, Theng, & Mora, 2010) and acidic conditions can also lead to the hydrolysis of side-chains and the hydrolysis of the acid-labile linkages between the GalA and Rha residues in the RG-I region (Khalikov & Mukhiddinov, 2004; Levigne, Ralet, & Thibault, 2002). Such acid-catalyzed hydrolysis can significantly impact both bioactivity (Li, Li, & Gao, 2014) and gel forming properties.

Non-metal Fenton chemistry is emerging as an alternative technology for the efficient degradation of chemically stable, organic substrates. These systems operate at near-ambient temperatures and pressures and also generate strongly oxidizing radical species (primarily HO•). The key non-metal Fenton-like chemistries include H_2O_2/ascorbic acid and H_2O_2/ozone (O_3). Although the H_2O_2/ozone (O_3) system can also degrade organic substrates with high efficiency, the high cost of O_3 and its toxicity in humans precludes its use. In comparison, the cost of H_2O_2/ascorbic acid system is much lower and these reagents are currently used within the food industry. The polysaccharide degradation efficiency, using a H_2O_2/ascorbic acid system, is comparable to that of metal catalyzed Fenton system (Verma, Baldrian, & Nerud, 2003). In addition, the H_2O_2/ascorbic acid system is eco-friendly and these reagents are easy to remove, can work in the absence of trace metal and can act over a broad pH range. In our previous study, we demonstrated that ultrasound enhances the efficiency of the metal-catalyzed Fenton reaction in degrading PPs and we elucidated the relevant mechanism (Zhi et al., 2017). However, it is still unclear whether ultrasound can accelerate the polysaccharide degradation efficiency of the non-metal Fenton chemistry.

The present study establishes ultrasound-accelerated non-metal Fenton-like chemistry (H_2O_2/ascorbic acid) to depolymerize PPs from citrus canning processing water, with aim of improving degradation efficiency. A mechanism is proposed for the efficient degradation of PPs by non-metal Fenton-like chemistry. The influence of ascorbic acid concentration, the sonolysis intensities, the reaction temperature, and the combined effect of sonolysis with H_2O_2/ascorbic acid redox system on the molecular weight were determined. The structural properties of the resulting LMPs were characterized by Fourier transform-infrared (FT-IR), nuclear magnetic resonance (NMR) spectroscopy and monosaccharide composition analysis. In addition, the *in vitro* tumor cell growth inhibitory effects and cytotoxicity of PPs and LMPs, were evaluated on MCF-7 human breast adenocarcinoma cells using 3-(4,5-dimethylthiazol-2-yl)-2,5-diphenyltetrazolium bromide (MTT) assay and lactate dehydrogenase (LDH) assay.

2. Materials and methods

2.1. Materials

The basic water discharged from citrus canning factories during the segment membrane removal process, was collected from citrus fruit canning factories (Ningbo, China). Gel-filtration column Ultrahydrogel 250 and TSK-Gel G 4000 SWXL column was from Waters and Tosoh Biosep, respectively. Hydrogen peroxide, ascorbic acid, HPLC-grade methyl alcohol and deuterium oxide were obtained from Sinopharm Chemical Reagent Co., Ltd. (Shanghai, China). The 95% (v/v) ethanol (food grade) and other chemical reagent were acquired from Aladdin Chemical Reagent Co., Ltd. (Shanghai, China).

2.2. Pectic polysaccharide recovery

Pectic polysaccharide was prepared following a previously reported method (Ye, 2017). Polysaccharide recovery initially involves a two-step filtration process with 200 and 400 meshes filters (size: $\Phi \times h = 1\,m \times 2\,m$) used to eliminate the suspended solid particles. The filtrate is then pumped (13 m^3/h, 11 kW) to the pH adjustment reactor (volume: 8 m^3, stirring power: 4 kW) for neutralization, followed by vacuum concentration (size: 5 m × 6 m × 9 m, 40 kW) at 70 °C. Precipitation (volume: 4 m^3, stirring power: 2 kW) with ethanol at a final ethanol concentration of 50 vol % was performed with gentle stirring. After standing for 30 min, the precipitation was completed and a screw machine (size: 3 m × 0.6 m × 2 m, 0.75 kW) was applied to recover the precipitates, which were the polysaccharides (insoluble in ethanol solution), and the filtrate was then transported to the alcohol recovery unit (integrated with the concentration unit, 12 kW). The precipitate was washed once with 95% ethanol and again ethanol recovered. Subsequently, vacuum drying (size: 1.5 m × 1.5 m × 1.7 m, 5 kW) was conducted on the precipitate (also with ethanol recovery). The dry polysaccharide was ground into a powder to obtain PPs.

2.3. Synergistic effect of ultrasonolysis and H_2O_2/ascorbic acid for depolymerization of pectic polysaccharide

Ultrasound treatments were performed (Scientz-IID, Ningbo Scientz Biotechnology Co., Ningbo, China) with the following parameters: maximum ultrasound power output, 900 W, frequency, 22 kHz, intermittent type, 2 s on and 2 s off, and horn micro tip diameter, 10 mm. Twenty-five milliliters of PPs solution (5 mg/mL) were placed in a cylindrical glass reactor (Φ, 2.90 cm) and the generator probe was submerged (about 1 cm below the liquid surface) to release ultrasonic energy.

Under the selected conditions, ultrasound/H_2O_2/ascorbic acid (ultrasonic intensity, 3.8 W/mL, the concentration of ascorbic acid, 10 mM and the concentration of H_2O_2, 50 mM), the results were compared with: single ultrasound treatments (3.8 W/mL), ultrasound (ultrasonic intensity, 3.8 W/mL) assisted with H_2O_2 (50 mM), ultrasound (ultrasonic intensity, 3.8 W/mL) assisted with ascorbic acid (10 mM), single H_2O_2 (50 mM), single ascorbic acid (10 mM), single H_2O_2/ascorbic acid system (the concentration of H_2O_2, 50 mM and the concentration of ascorbic acid, 10 mM). All the tests were performed at the temperature of 30 °C for 60 min.

2.4. Effect of reaction conditions on the molecular weights (Mw) of depolymerized product

The effects of the following parameters were investigated: ultrasound intensity (3.8, 7.6, 11.4 and 15.2 W/mL), temperature (20, 30, 40 and 50 °C) and ascorbic acid concentration (1.0, 10, 50 and 100 mM). The general depolymerization conditions of all treatments were as follow: reaction time of 60 min, temperature at 30 °C, ascorbic acid concentration of 10 mM, hydrogen peroxide of 50 mM, the ultrasound intensity of 3.8 W/mL. The Mw of pectin samples were determined by gel permeation chromatography (GPC) according to our previously studies, with some modifications (Guo et al., 2014). The average Mw determination was performed on a LC-20A HPLC system (Shimadzu, Kyoto, Japan) with an Ultrahydrogel 250 column (Waters, Milford, USA). Forty microliters of the sample solution were injected and eluted by 0.2 M NaCl at a flow rate of 0.5 mL/min. Standard dextrans (Sigma-Aldrich Chemical Co., St. Louis, MO, USA) having different molecular weights (from 0.5 to 670 kDa) were used to obtain calibration curves.

2.5. Estimation of hydroxyl radicals

A method, based on the reaction of deoxyribose with HO• radicals (Verma et al., 2003), was used for the study of the time course of production of HO• radicals by the optimized ultrasound/H_2O_2/ascorbic acid system. Aliquots of the reaction mixture (450 μL) were taken at different time intervals and supplemented with 50 μL deoxyribose (28 mM). The reaction was stopped by the addition of 500 μL thiobarbituric acid (1% w/v in 50 mM NaOH) and 500 μL of trichloroacetic acid (2.8% w/v) after 5 min of incubation. The deoxyribose degradation product reacted with thiobarbituric acid during a subsequent 30 min incubation at 80 °C, with the resulting formation of a pink compound. The product of the reaction was quantified by spectrophotometry (λ = 532 nm) after dilution with an equal amount of water. The relative amount of HO• radicals detected was expressed in absorbance units.

2.6. Determination of hydroxyl radicals by ESR spin-trapping technique

ESR measurements were performed on an X-band ESR spectrometer (JES-FA-200; JEOL, Tokyo, Japan) at room temperature. The measurement conditions were as follows: field sweep, 317.7–327.7 mT; field modulation frequency, 100 kHz; field modulation width, 0.1 mT; amplitude, 2; sweep time, 4 min; time constant, 0.03 s; microwave frequency, 9.054 GHz; microwave power, 0.998 mW. All experiments were performed in triplicate at room temperature.

2.7. Determination of monosaccharide composition

Monosaccharide composition of oligosaccharide fragments was determined by the 1-phenyl-3-methyl-5-pyrazolone (PMP) high performance liquid chromatography (HPLC) method (Wu et al., 2013). Briefly, approximately 2 mg of pectin samples was hydrolyzed with 4 M trifluoroacetic acid (TFA) at 110 °C for 8 h. After cooling to room temperature, TFA was then removed and the reaction solution was adjusted to pH 7.0 with 2 M NaOH, and then with 0.3 M NaOH. The hydrolysate was derivatized with 50 μL of 0.3 M NaOH and 50 μL of 0.5 M PMP solution at 70 °C for 100 min. Chloroform was used to extract the hydrolysate and the hydrolysate was analyzed by a Waters 2695 HPLC system (Waters, USA) with an ZORBAX Eclipse XDB-C18 column (Agilent, 5 μm, 4.6 mm × 250 mm, Santa Clara, CA, USA). Mobile phase A was aqueous containing sodium phosphate buffer (0.05 M, pH 6.9) and acetonitrile (v/v; 85:15) and mobile phase B was aqueous containing sodium phosphate buffer (0.05 M, pH 6.9) and acetonitrile (v/v; 60:40). The time program of HPLC analysis was 0 → 10→30 min and the concentration program was 0 → 8%→20% of the mobile phase B at a flow rate of 1 mL/min and the samples were detected by UV detection at 250 nm, and the injection volume was 20 μL.

2.8. IR spectral analysis

The FT-IR analysis was applied to obtain IR spectra of the pectin samples using a Nicolet Avatar 370 instrument. Samples (~1 mg) were ground together with 200 mg KBr, pressed into pellets for IR scanning from 400 to 4000 cm^{-1} with 32 scans and a 4 cm^{-1} resolution. The degree of esterification and other functional groups were determined.

2.9. NMR analysis of low-molecular-weight pectin

For NMR analysis, citrus pectin and LMP fractions (~5 mg) were evaporated with 550 μL of D_2O (99.96%) twice by vacuum freeze drying before final dissolution in 550 μL of D_2O (99.96%). The samples were acquired in D_2O with chemical shifts expressed as δ PPM, using the resonances of CH_3 groups of acetone (δ 30.2/2.22) as internal reference. NMR spectra were collected by a 600 MHz NMR spectrometer (DD2-600; Agilent Technologies Inc., CA, US) at 25 °C. The spectra were processed using the MestReNova 6.1.1 (MestreLab Research, Santiago de Compostela, Spain).

2.10. Cell viability assay

The antitumor activity of PPs and LMWP on MCF-7 cells was evaluated using the tetrazolium salt 3-(4,5-dimethylthiazol-2-yl)-2,5-diphenyltetrazolium bromide (MTT) assay (Miao et al., 2013). The cells were incubated in Dulbecco's modified eagle medium (DMEM) supplemented with 10% fatal bovine serun (FBS), 100 U/mL of penicillin and 100 g/mL of streptomycin at 37 °C in a humidified incubator at 5% CO_2. Briefly, 100 μL of the cells were incubated in a 96-well plate at a concentration of 2×10^5 cells/mL. After 24 h of cultivation, various concentrations of PPs and LMP (0, 10, 50, 100, 250 and 500 μg/mL) were added slowly into the 96-well plate and cultured for 48 h. Fluorouracil (5-FU, 50 μg/mL) served as the positive control. At the end of each treatment, 20 μL of MTT (5 mg/mL) was added and the tumor cells were further incubated for 4 h for the formation of the formazan crystals. A volume of 100 μL DMSO was added to each well to dissolve the formazan crystals after the medium was removed. Subsequently, absorbance was measured at 570 nm with a microplate reader (Thermo multiscan Mk3, Thermo Fisher Scientific Inc., USA). The cell viability was expressed as

$$\text{Cell viability (\% control)} = [(A_s - A_b)/(A_c - A_b)] \times 100$$

where A_c and A_b were the absorbance of the system without the addition of polysaccharides or 5-FU and cells, respectively, and As was the absorbance of the system only with polysaccharides or 5-FU.

2.11. Lactate dehydrogenase (LDH) assay

The cytotoxicity of the samples was assessed by measuring the release of lactate dehydrogenase (LDH) into the culture medium as an indicator of cell membrane injury 30 using a commercial LDH assay kit (Jiancheng BioEngineering, Nanjing, China) according to manufacturer's instructions. Briefly, at the end of the incubation period, 20 μL supernatant of the culture medium from different treatments was used to assess LDH leakage into the media. Subsequently, absorbance was measured at 440 nm with a microplate reader (Thermo multiskan Mk3, Thermo Fisher Scientific Inc., USA). The LDH release ratio (% control) was expressed as;

$$\text{LDH release ratio (\% control)} = [(A_s - A_b)/(A_c - A_b)] \times 100$$

where A_c and A_b were the absorbance of the system without the addition of polysaccharides or 5-FU and cells, respectively, and As was the

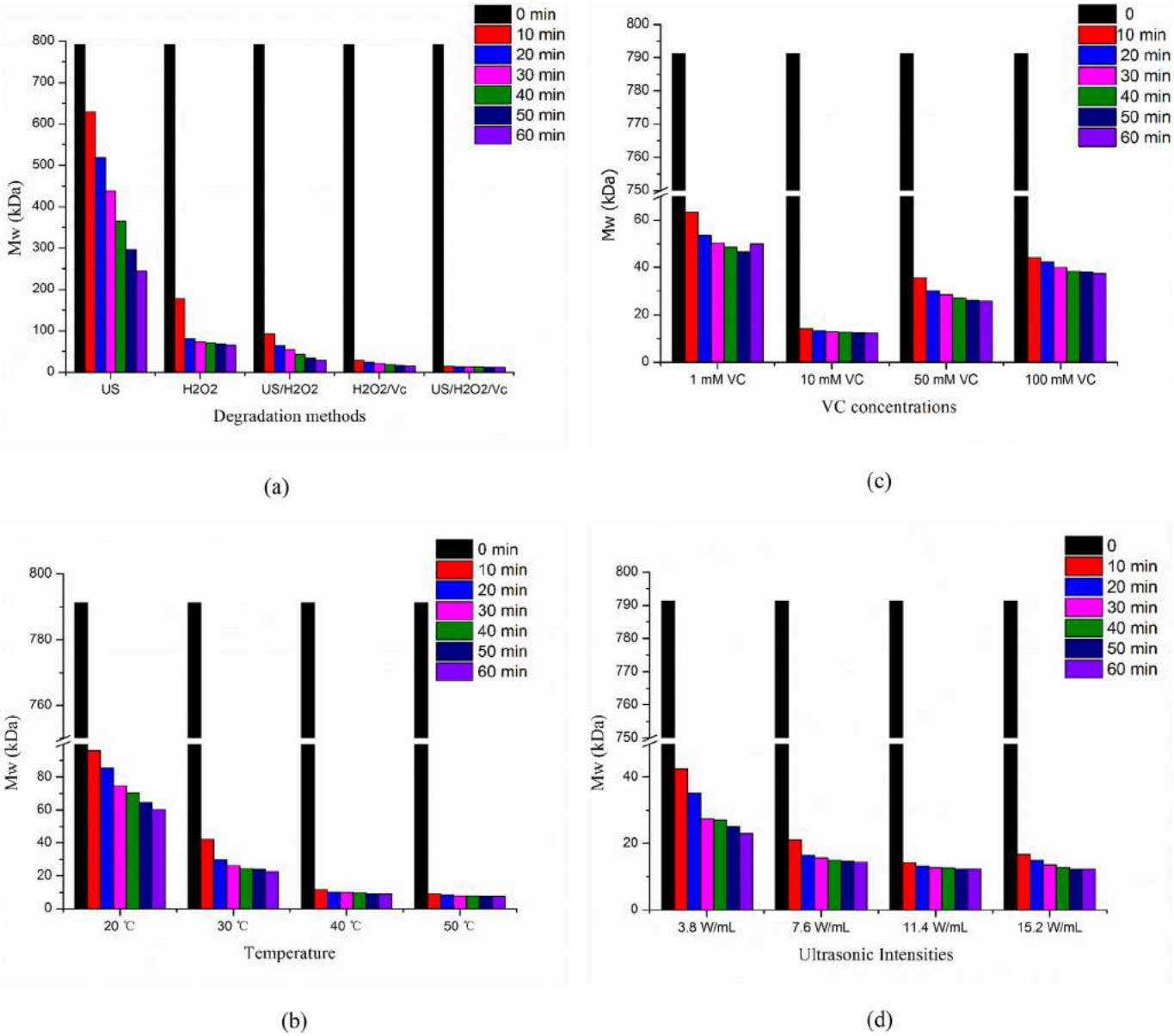

Fig. 1. Effect of different reaction conditions on the molecular weights of depolymerized pectic polysaccharides: (a) different degradation systems (ultrasound alone; H_2O_2 alone; ultrasound in combination with H_2O_2; H_2O_2/ascorbic acid redox system; ultrasound in combination with H_2O_2/ascorbic acid system); (b) reaction temperature (temperature, 20 °C, 30 °C, 40 °C or 50 °C; H_2O_2 concentration, 50 mM; ascorbic acid concentration, 10 mM; ultrasound intensity, 3.8 W/mL); (c) ascorbic acid concentration (1 mM, 10 mM, 20 mM or 100 mM; H_2O_2 concentration, 50 mM; temperature, 30 °C; ultrasound intensity, 3.8 W/mL); (d) ultrasound intensity (intensity, 3.8 W/mL, 7.6 W/mL, 11.4 W/mL or 15.2 W/mL; H_2O_2 concentration, 50 mM; ascorbic acid concentration, 10 mM, temperature, 30 °C).

absorbance of the system only with polysaccharides or 5-FU.

3. Results and discussion

3.1. The synergetic effects of sonolysis and H_2O_2/ascorbic acid system to depolymerize pectic polysaccharide

We first examined whether H_2O_2/ascorbic acid each used on its own could depolymerize PPs. The results (Fig. 1a) suggested H_2O_2/ascorbic acid could depolymerize PPs and reduce their average molecular weight from 791 kDa to 15.27 kDa in 60 min. In stark contrast, a 60 min treatment with ultrasound or H_2O_2 alone resulted in no apparent reduction of molecular weight. Interestingly, when H_2O_2 was combined with ultrasound the molecular weight of pectin polysaccharides could be reduced to below 20 kDa. These results suggest that while H_2O_2/ascorbic acid system is an efficient system to generate LMPs, ultrasound enhances the efficiency of free radical depolymerization.

Further studies on ultrasound enhanced H_2O_2/ascorbic acid depolymerize PPs showed that not only that the degradation process was accelerated but also the degradation efficiency was greatly improved with the appearance of 14.26 kDa products within 10 min.

3.2. Effects of reaction parameters on pectic polysaccharide depolymerization

The effect of reaction temperature, ascorbic acid concentration, and ultrasonic intensity during the depolymerization process on the degradation efficiency was examined to optimize the depolymerization conditions. A neutral pH was applied in the present study to prevent the acidic or basic hydrolysis of the polysaccharides, as the branching chain may important for the activity of the PPs.

Increased temperatures result in higher average kinetic energy as a

result of more molecular collisions per unit time (Yue et al., 2008). Furthermore, cavitation bubbles formed during the ultrasonic treatment can degrade organics (Golash & Gogate, 2012). As a result, degradation efficiency increased markedly by elevating the reaction temperature from 20 to 40 °C (Fig. 1b). However, no obvious improvement in degradation efficiency was observed when the temperature was increased to 50 °C. At high temperatures, the concentrations of both H_2O_2 and ascorbic acid can be reduced due to their self-decomposition, thus, decreasing degradation efficiency. Therefore, 40 °C was selected as the optimal reaction temperature.

Reaction rates accelerate with the increasing concentrations of reactants. When the concentration of H_2O_2 was 50 mM, increasing ascorbic acid concentration from 1 to 10 mM increased the degradation efficiency due to the increasing amount of HO•. Nevertheless, when the ratio of the concentration of H_2O_2 to the concentration of ascorbic acid was < 5, higher concentrations of ascorbic acid (> 10 mM) were not effective for the depolymerization of PPs (Fig. 1c). Under these reaction conditions, excess ascorbic acid (H_2A) is susceptible to autoxidation to generate dehydroascorbic acid anions (Eqs. (1) and (2)) that react with HO•, generated from H_2O_2/ascorbic acid redox system (Eq. (3)), (Bai & Wang, 1998) resulting in a decrease in depolymerization efficiency. Therefore, 10 mM ascorbic acid was considered as the appropriable concentration.

$$H_2A \rightarrow HA^- + H \quad (1)$$

$$HA^- + O_2 \rightarrow A^-\bullet + O_2^- + H^+ \quad (2)$$

$$HA^- + HO\bullet \rightarrow A^-\bullet + H_2O \quad (3)$$

Ultrasound intensity has been used as an important operational parameter in ultrasonic processes for controlling the formation of HO• radicals and cavitation bubbles (Joseph, Puma, Bono, & Krishnaiah, 2009). Degradation efficiency increases with increasing ultrasound intensities from 3.8 to 11.4 W/mL (Fig. 1d). Nevertheless, no further obvious improvement was detected when the ultrasound intensity was increased to 15.2 W/mL. In contrast to the ultrasound in the metal-catalyzed Fenton chemistry for pectin depolymerization, which mainly functions as a catalyst accelerating pectin depolymerization (Zhi et al., 2017), the ultrasound (3.8–11.4 W/mL) in the H_2O_2/ascorbic acid system ultrasound reaction acts as both a catalyst, accelerating the generation of free radicals, and also significantly changes the end point of the reaction. Ultrasound of 11.4 W/mL was selected as a suitable value to maximize conversion.

Based on results obtained, we set the optimal values of 40 °C, 10 mM, 11.4 W/mL as our reaction conditions. Ultrasound/H_2O_2/ascorbic acid was used to generate hydroxyl radicals in subsequent experiments. The involvement of hydroxyl radicals during PPs depolymerization is similar to the depolymerization of PPs by copper (II) and hydrogen peroxide. Hydroxyl radicals react with PPs by abstracting a hydrogen atom, leading to the sugar chain scission (Zhi et al., 2017).

3.3. Estimation of hydroxyl radicals

Ultrasound/H_2O_2/ascorbic acid is an effective and environmentally friendly method to depolymerize PPs. The system produces hydroxyl radicals during the reaction and the involvement of hydroxyl radicals during the depolymerization of PPs is similar to decolorization of dyes by ascorbic acid, copper (II) and hydrogen peroxide (Verma et al., 2003). HO· radicals have an unpaired electron making them strong oxidizing agents that react with polysaccharides causing their degradation. The concentration of HO· radicals in the ultrasound/H_2O_2/ascorbic acid system is the highest during the reaction, which explains the efficient degradation of PPs under these conditions (Fig. 2). The concentration of HO· radicals in the absence of ultrasound is obviously lower than that observed in the ultrasound/H_2O_2/ascorbic acid system. In the absence of ascorbic acid the amount of HO· radicals is considerably lower. It has been widely acknowledged that low frequency ultrasonic degradation of most water-soluble polymers in aqueous solutions is mainly attributed to the almost midpoint scission by mechanical effects induced by ultrasound (Koda, Taguchi, & Futamura, 2011). Our results indicate that low frequency ultrasound can also act as special catalyst to speed up and increase the total production of HO· radicals using non-metal Fenton chemistry, resulting in higher PPs depolymerization.

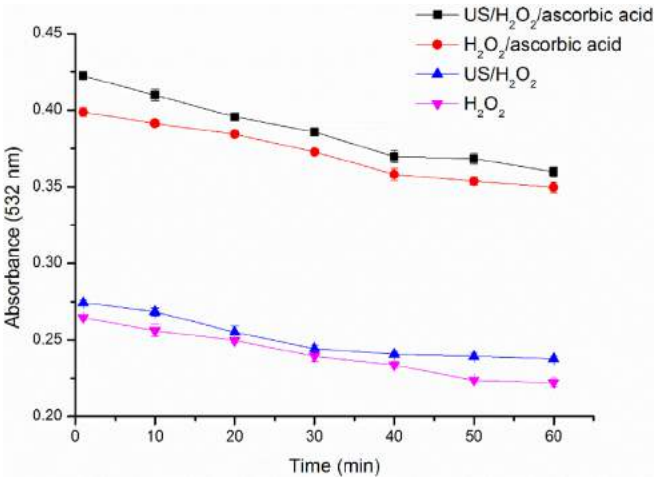

Fig. 2. Concentrations of hydroxyl radicals during the incubation of H_2O_2 (50 mM) + ascorbic acid (10 mM)/H_2O_2 (50 mM) in the presence and absence of ultrasound (11.4 W/mL). The concentration is expressed as absorbance of the deoxyribose degradation product with thiobarbituric acid.

Electron spin resonance (ESR) technique was employed to detect HO· in the different reaction systems. The spin adduct 5,5-dimethyl-1-pyrroline N-oxide (DMPO)-OH, an adduct of DMPO and the hydroxyl radicals, was assigned based on hyperfine coupling constants (hfcc). The hfcc are aH = aN = 1.49 mT, which is consistent with those of previous reports (Mokudai, Nakamura, Kanno, & Niwano, 2012). Relatively weak signals from DMPO-OH were detected in both H_2O_2 and ultrasonic/H_2O_2 systems (Fig. 3). The addition of ascorbic acid resulted in the appearance of a strong signal from DMPO-OH and further increase of ultrasound energy enhanced the signal from DMPO-OH. These ESR spectra suggest that the amount of hydroxyl radical produced by the H_2O_2/ascorbic acid system was significantly higher than that of

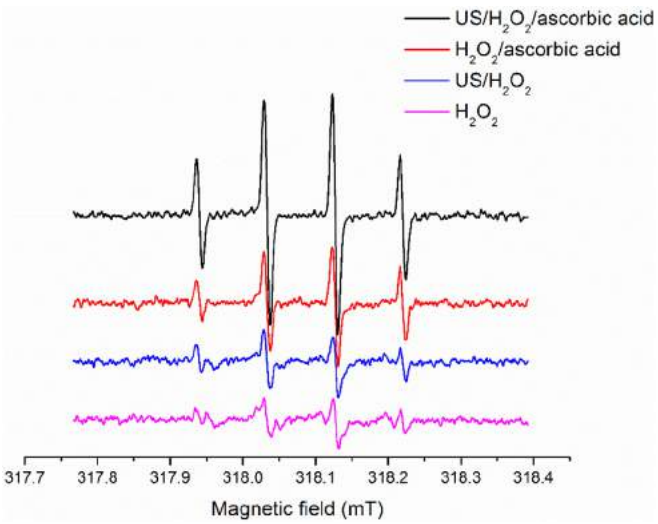

Fig. 3. ESR spectra of reaction solution under different systems. H_2O_2 (50 mM); US (11.4 W/mL)/H_2O_2 (50 mM); H_2O_2 (50 mM)/ascorbic acid (10 mM); US (11.4 W/mL)/H_2O_2 (50 mM)/ascorbic acid (10 mM).

H_2O_2 alone or ultrasound/H_2O_2 and that ultrasound could increase the concentration of hydroxyl radicals in the H_2O_2/ascorbic acid system. These data are consistent with the hydroxyl radical concentration estimated in the assay above.

3.4. Monosaccharide composition analysis

During the optimization process, three forms of degraded PPs with distinct molecular weights were obtained. PPs were depolymerized under optimized conditions from 791 kDa to 12.26 kDa (LMP2) within 60 min. Under milder (20 °C, 10 mM, 11.4 W/mL) and more severe (50 °C, 10 mM, 11.4 W/mL) conditions, relatively higher molecular weight (60.33 kDa) (LMP1) and lower molecular weight (7.65 kDa) (LMP3) products were obtained, respectively.

Chemical compositional analysis indicated that GalA (in mole%) was the principle component of the four polysaccharides, while arabinose (Ara) and galactose (Gal) were the major neutral saccharides. All chemical compositions, determined in the native PPs, were also detected in each of the three depolymerized products, suggesting that ultrasound/H_2O_2/ascorbic acid system did not alter the types of monosaccharides present. With decreased molecular weights the total mole percentage of neutral monosaccharides increased and the GalA content decreased (Table 1), suggesting that chain breakage might occur at GalA residues.

All four samples were relatively rich in homogalacturonans (HG) as opposed to rhamnogalacturonans (RG), as deduced from the Rha/GalA ratio (Arnous & Meyer, 2009). The low ratio of 0.51 determined for the native PPs indicates that both the homogalacturonans and rhamnogalacturonans are predominate, whereas the increasing ratio, close to 1, for three depolymerized products suggests that these contain a majority of rhamnogalacturonan with a repeating unit of [→2)-α-L-Rha*p*-(1 → 4)-α-D-Gal*p*A-(1→] (where *p* is pyranose). The ratio of (Ara + Gal) to Rha was calculated to estimate the relative importance of the neutral side-chains to the rhamnogalacturonan backbone. These ratios were at 5.48, 5.32, 5.04, 4.96 for PP, LMP1, LMP2 and LMP3, respectively. The ratios Rha/GalA and (Ara + Gal)/Rha indicate that free radicals generated preferentially attack GalA residues in the HG region of PPs, which was similar to the reported preference for free radical depolymerization of pectin catalyzed by ultrasound-Fenton chemistry (Zhi et al., 2017). Thus, this method might be applicable for the rapid preparation of RG-I enriched LMPs.

3.5. Degradation products analysis by IR

The infrared spectra of the four samples are provided in Fig. 4. Both native PPs and its depolymerized products display similar spectral bands as IR is relatively insensitive to minor structural changes in large polymer molecules. The major absorption at around 3405 cm^{-1} can be attributed to stretching of hydroxyl groups. The peak at around 3422 cm^{-1} corresponds to C–H absorption, including CH, CH_2 and CH_3 stretching and bending vibrations and an absorption at 2932 cm^{-1} is assigned to CH stretching of CH_2 groups. The degree of methylation (DM) of pectin can be estimated by dividing the signal ascribed to carboxylic ester by the sum of the signal ascribed to carboxylic ester and carboxylic acid groups (Fellah, Anjukandi, Waterland, & Williams, 2009; Gnanasambandam & Proctor, 2000). Signals at 1609 cm^{-1} can be attributed to the C = O stretching vibration of ionic carboxyl groups and no absorption corresponding to carboxylic ester could be found, indicating the absence of esterified pectins. The three absorption peaks between 1010 and 1150 cm^{-1} indicated the presence of pyranose (Zhang et al., 2013) and the pyranose configuration of the pectin did not change after ultrasound/H_2O_2/ascorbic acid treatment.

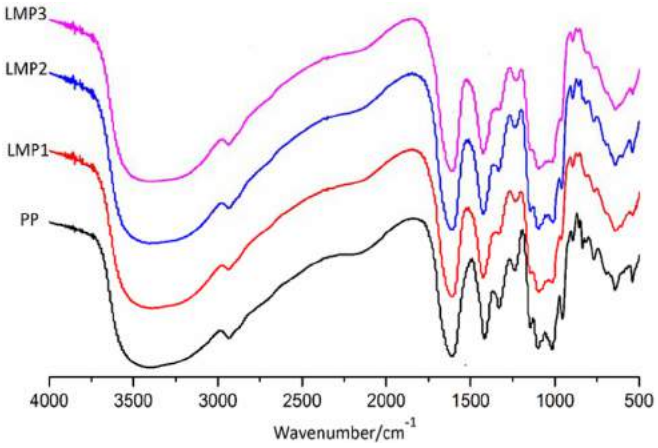

Fig. 4. IR spectra (% transmittance as a function wavenumber) of native PPs and LMPs prepared by ultrasound/H_2O_2/ascorbic acid process. LMP1, LMP2 and LMP3 were prepared by US/H_2O_2/ascorbic acid system (ultrasound intensity, 11.4 W/mL; H_2O_2 concentration, 50 mM; ascorbic acid concentration, 10 mM) in 20 °C, 30 °C and 50 °C, respectively.

3.6. NMR spectra

The ^{1}H NMR spectra of PP, LMP1, LMP2 and LMP3 were obtained to better understand the structural change of PPs during oxidation (Fig. 5). In comparison, the depolymerized pectins exhibited similar spectra to the native polysaccharides, containing characteristic signals. Specifically, the signals at 1.31 ppm and 1.24 ppm were derived from methyl groups of L-rhamnose and were assigned to the *O*-2- and *O*-2,4-linked rhamnose, respectively (Zhi et al., 2017). In the anomeric region, the signals from 5.05 to 5.3 ppm correspond to the anomeric protons of Ara and signals at 5.29 ppm and 4.67 ppm were assigned to the H-1 of Rha and H-1 of Gal, respectively.

Some changes were observed following depolymerization. Signals at 4.01 ppm and 4.46 ppm, assigned to the H-3 and H-4 of GalA, respectively, showed a substantial decrease in intensity under more stringent reaction conditions, suggesting the selective cleavage of GalA. These results are in agreement with those from the monosaccharide compositional assay (Section 3.4). Thus, based on the ^{1}H NMR data, it can be reasonably inferred that the reaction temperature is the most important factor in the system and HO·generated by ultrasound/H_2O_2/ascorbic acid process selectively attacks the glycosidic bond without damaging

Table 1
Monosaccharide composition of different pectin polysaccharides.

Monosaccharides (mol%)	PPs	LMP1	LMP2	LMP3
Ara	44.55 ± 1.08	47.95 ± 1.14	47.46 ± 1.33	48.2 ± 1.46
GalA	22.3 ± 0.92	17.32 ± 0.86	15.43 ± 0.68	14.36 ± 0.63
Gal	18.4 ± 0.24	18.74 ± 0.18	18.82 ± 0.36	18.58 ± 0.16
Rha	11.49 ± 0.08	12.54 ± 0.24	13.16 ± 0.13	13.46 ± 0.09
Fuc	2.3 ± 0.16	2.34 ± 0.08	3.91 ± 0.28	4.22 ± 0.11
Xyl	0.91 ± 0.03	1.11 ± 0.05	1.22 ± 0.08	1.18 ± 0.14
(Ara + Gal)/Rha	5.48	5.32	5.04	4.96
Rha/GalA	0.512	0.72	0.85	0.94

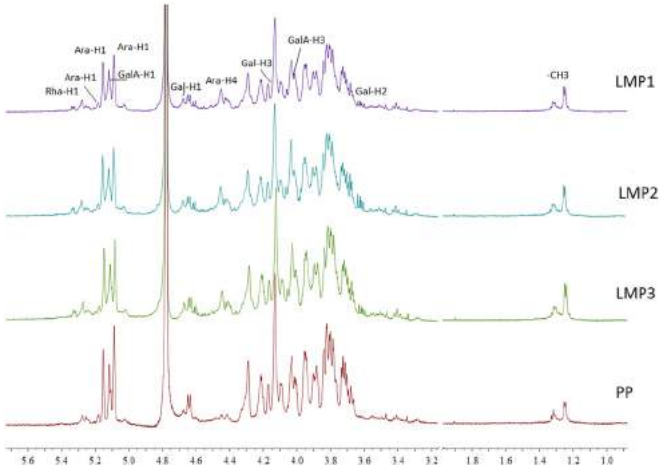

Fig. 5. ^{1}H NMR spectra (intensity and a function of chemical shift in ppm) of PPs and LMPs. LMP1, LMP2 and LMP3 were prepared by US/H_2O_2/ascorbic acid system (ultrasound intensity, 11.4 W/mL; H_2O_2 concentration, 50 mM; ascorbic acid concentration, 10 mM) in 20 °C, 30 °C and 50 °C, respectively.

the RG-I region of PPs, similar to metal-catalyzed Fenton chemistry (Bokare & Choi, 2014).

Due to the limited resolution of the ^{1}H NMR spectra of the polysaccharide mixtures, 2D NMR was employed to further determine the structure of LMP3 as a representative product. The assignments of ^{1}H and ^{13}C chemical shifts (Table 2) were made from total correlation spectroscopy (TOCSY) (Fig. 6a), heteronuclear single quantum coherence (HSQC) spectra (Fig. 6b) and nuclear Overhauser effect spectroscopy (NOESY) (Fig. 6c). The analysis of the COSY and TOCSY revealed the residues with α- and β-galactopyranosidic, α-rhamnopyranosidic and α-arabinofuranosidic configuration. The HSQC spectrum showed that the residue with α-galacto-configuration corresponded to the α-galactopyranosyl uronic acid residues substituted at position 4 (Bushneva, Ovodova, Shashkov, & Ovodov, 2002) and α-arabinofuranosidic residues were both non-substituted C5 (64.81 ppm) and 5-subsituted (C5 72.5 ppm). The correlation peak of H1/H4 (5.12/4.46) of the GalA residues in the NOESY spectrum further confirmed the presence of α-1,4-linked galactopyranosyl uronic acid residues. The correlation peaks of H1(Gal*p*A)/H2(Rha*p*) at 5.12/4.32 ppm, H1(Ara*f*)/H4(Rha*p*) (where *f* is furanose) at 5.14/4.45 ppm and H1(Gal*p*)/H4(Rha*p*) at 4.67/4.45 ppm in NOESY spectra indicated that some GalA residues are linked to the 2-position of Rha residues and some Ara*f* and Gal*p* residues are linked to the 4-position of Rha residues. In addition, the correlation peak of H1(Rha*p*)/H4(Gal*p*A) at 5.29/4.46 ppm confirmed that the residues of rhamnopyranose are linked to the 4-position of α-GalA residues. Observation of correlation signals B1/B5 at 5.11/3.93 in the NOESY spectrum suggested the presence of a fragment … →5)-Ara*f*-(1 →5)-Ara*f*-(1 → …. Correlation signal at D1/C3 (5.27/4.15 ppm) led to an unambiguous identification of substitution of residue (C) by terminal *α*-Ara*f* at C3.

Because LMP3 is a LMP mixture it is not possible to assign all of the signals in NMR spectra. Based on the data obtained, we suggested that the core of the pectic polysaccharide is composed of residues of α-1,4-galactopyranosyl uronic acid and α-1,2-rhamnopyranose. The side chain of hair regions was represent different blocks composed of residues of α-1,5- linked arabinofuranose and as well as β-1,4- linked galactopyranose, consistent with previous reports that neutral fragments of arabinan and galactan are the most likely the side chain of pectic polysaccharides attached to the backbone of rhamnogalacturonan (Bushneva et al., 2002). Arabinogalactans (AG I, AG II) and possibly galactoarabinans are also typical neutral sugar side chains of branched RG I polysaccharides. The presence of β-1,3-linked-Gal*p* units also suggests the presence of arabinogalactans in LMP3 (Carlotto et al., 2016).

3.7. *The proposed mechanism of pectic polysaccharide depolymerization by ultrasound/H_2O_2/ascorbic acid system*

Based on the detailed analysis of chemical composition, IR and NMR, the mechanism of ultrasound/H_2O_2/ascorbic acid process to generate RG-I enriched fragments can be proposed (Fig. 7). The radical degradation process occurs through generation of free hydroxyl radical OH·by ultrasound/H_2O_2/ascorbic acid system. Ultrasound induces acoustic cavitation and the subsequent violent collapse of cavitation at multiple locations in the system can increase the temperature (about 5000 K) and pressures (2000 atm) significantly in the collapsing bubble and close vicinity of the bubble, which gives rise to generation of OH· and H· radicals, which can subsequently form hydrogen peroxide (H_2O_2) (Eqs. (4)–(8)) (Czechowska-Biskup, Rokita, Lotfy, Ulanski, & Rosiak, 2005; Gogate & Prajapat, 2015; Leonelli & Mason, 2010), resulting in an additive effect of ultrasonic treatment and H_2O_2/ascorbic acid redox system, generating more HO• radicals. In addition, the

Table 2
1H/13C NMR chemical shifts assignments of LMP3.

Residue	Chemical shift (ppm)					
	H1	H2	H3	H4	H5	H6
	(C1)	(C2)	(C3)	(C4)	(C5)	(C6)
→3)-α-Ara-(1→ A	5.17	4.47	4.11	4.15	3.77/3.83	–
	(111.18)	(81.39)	(80.15)	(84.69)	(64.81)	
→5)-α-Ara-(1→ B	5.11	4.31	4.13	4.19	3.83/3.93	–
	(111.20)	(85.32)	(84.69)	(81.29)	(72.50)	
→3,5)-α-Ara-(1→ C	5.14	4.41	4.15	4.45	3.83/3.95	–
	(110.97)	(80.55)	(85.99)	(81.74)	(72.66)	
α-Ara-(1 → 3 D	5.27	4.35	4.12	4.25	3.77/3.83	
	(113.67)	(81.74)	(86.36)	(85.99)	(68.37)	
→4)-α-GalA-(1→ E	5.12	3.95	4.01	4.46	4.69	–
	(102.67)	(69.92)	(72.39)	(81.39)	(73.40)	
→3)-β-Gal-(1→ F	4.65	3.69	4.18	4.29	3.72	3.75
	(107.98)	(76.02)	(85.05)	(74.05)	(78.22)	(64.73)
→4)-β-Gal-(1→ F′	4.67	3.59	3.77	4.43	3.72	3.75
	(107.98)	(77.06)	(72.05)	(80.96)	(78.22)	(64.73)
→2)→α-Rha-(1→ G	5.29	4.32	4.03	3.95	3.92	–
	(102.27)	(80.39)	(72.62)	(73.03)	(72.62)	
→2,4)-α-Rhap-(1→ G′	5.30	4.51	4.03	4.45	4.14	–
	(102.27)	(81.74)	(72.62)	(82.52)	(73.98)	

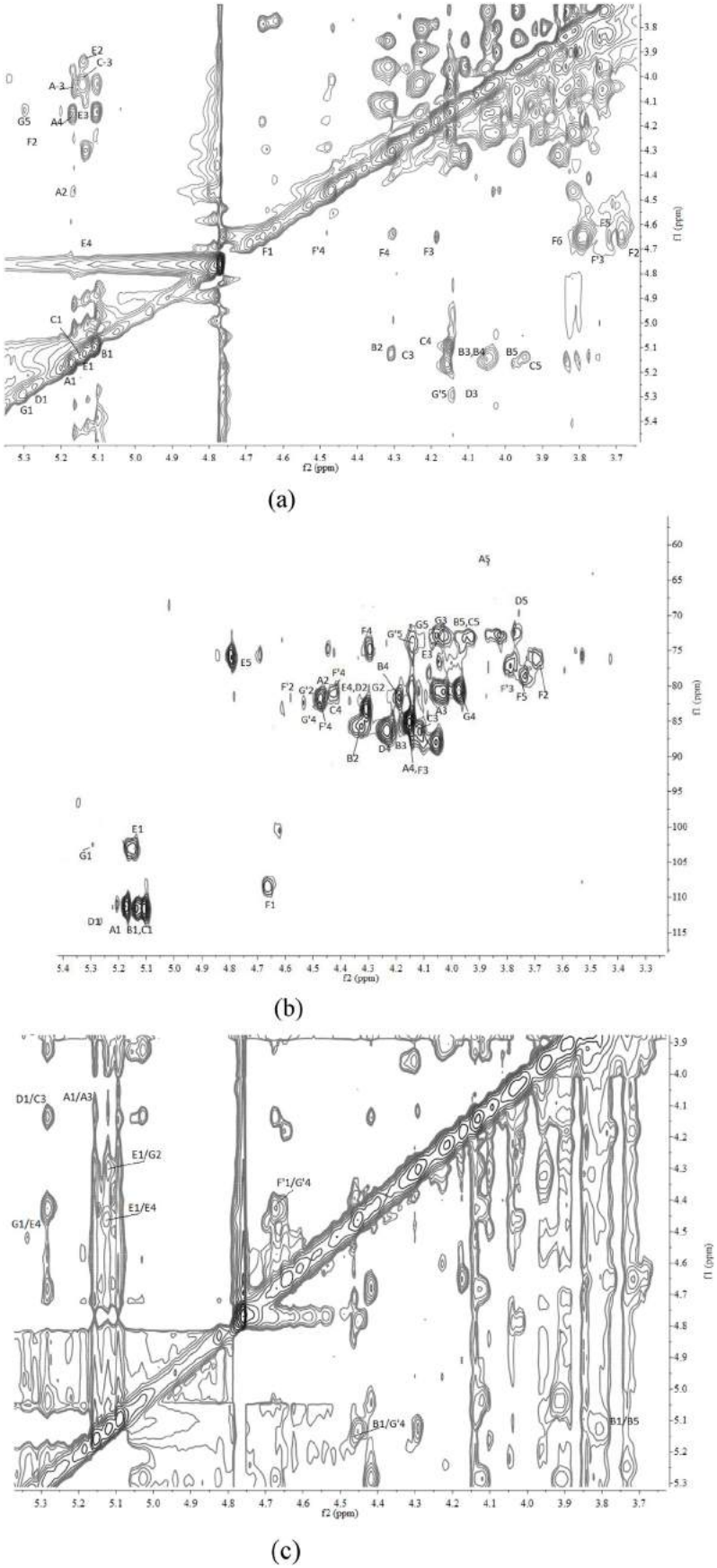

Fig. 6. NMR spectra of LMP3 (a) TOCSY of LMP3; (b) HSQC of LMP3; (c) NOESY of LMP3. LMP3 were prepared by ultrasonic/H_2O_2/ascorbic acid system (ultrasound intensity, 11.4 W/mL; H_2O_2 concentration, 50 mM; ascorbic acid concentration, 10 mM; reaction temperature: 50 °C).

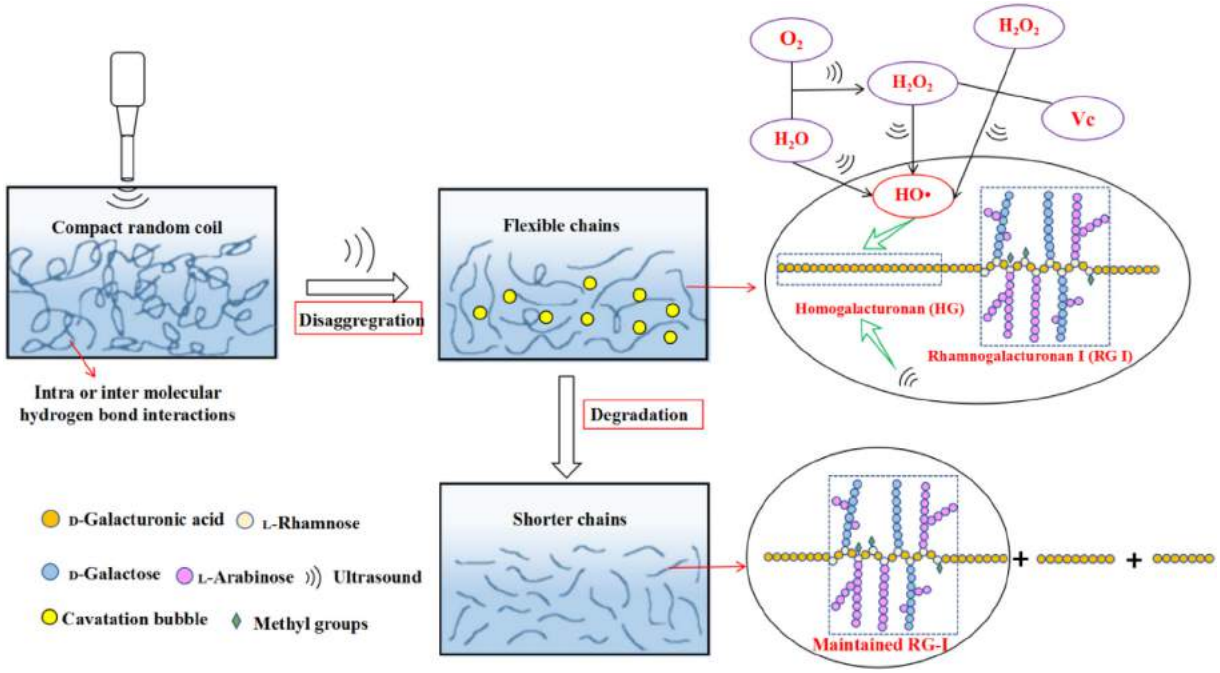

Fig. 7. The schematic diagram of PPs degradation path by ultrasound/H_2O_2/ascorbic acid system. The ultrasound enhances the efficiency of H_2O_2/ascorbic acid system to degrade PPs through both chemical effects (increasing the amount of hydroxyl radicals and lowering activation energy of H_2O_2 decomposition) and mechanical effects (disaggregating polysaccharide clusters).

ultrasound can also lower activation energy for H_2O_2 decomposition. The high temperature and pressures due to the significant release of accumulated energy and hot spots when the bubble collapse can significantly contribute to water ionization, leading to higher concentration of H^+ in the system (Eq. (9)) (Marshall & Franck, 1981). The H^+ can interact with carbonyl group (C=O) in the ascorbic acid and C1 becomes a positive carbon ion following the electron redistribution. Electronic cloud density distribution of C3 decreases the generation of extended pi bond with C1, thus, contributing to the complexation between C3 and hydroxyl groups of H_2O_2 and redox reactions (Eq. (10)). It also has been reported that ultrasound can depolymerize polysaccharide due to the physical effects (Zhang et al., 2013). During the ultrasound treatment, the shear force can lead to the disaggregation of polysaccharide clusters, especially in the early stage by breaking up the non-covalent intra and inter-molecular bonds (Yan, Pei, Ma, & Wang, 2015) and the resulting flexible structure makes the PPs more vulnerable to free radical attack. The reactive species primarily attacks at the glycosidic bond and the GalA residues on the HG domain are more reactive with hydroxyl radicals, resulting in chain scission and RG-I enriched fragments, which is consistent with previous reports that alduronic acid (GalA and GlcA, etc.) residues of polysaccharides are very susceptible to free radical degradation (Li et al., 2016; Uchiyama, Dobashi, Ohkouchi, & Nagasawa, 1990; Zhang et al., 2013; Zhi et al., 2017).

$$H_2O \rightleftarrows H\bullet + HO\bullet \quad (4)$$

$$H\cdot + O_2 \rightleftarrows HO_2\cdot \quad (5)$$

$$H\cdot + HO_2\cdot \rightleftarrows H_2O_2 \quad (6)$$

$$HO\bullet + HO\bullet \rightleftarrows H_2O_2 \quad (7)$$

$$HO_2\cdot + HO_2\cdot \rightleftarrows H_2O_2 + O_2 \quad (8)$$

$$H_2O \rightleftarrows H^+ + OH^- \quad (9)$$

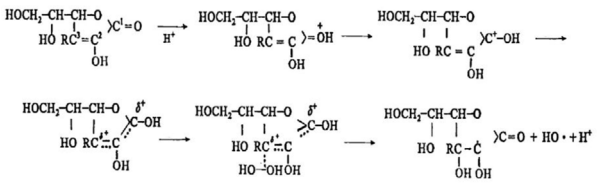

(10)

Free radical generation by ultrasound/H_2O_2/ascorbic acid system is also suitable for ultrafast preparation of other low molecular weight polymers and has been helpful in unraveling the structure of unknown polysaccharides.

3.8. Cell viability assay and cytotoxicity assay

The *in vitro* antitumor activity of both native PPs and LMP3 were determined at different concentration (0, 10, 50 100, 250, 500 μg/mL) by examining the proliferation of MCF-7 cells. LMP3 significantly inhibited the proliferation of MCF-7 cells and the inhibitory effect increased in a concentration-dependent manner (Fig. 8a). Intact PPs exhibited a much lower inhibitory effect on MCF-7 cells proliferation. LMP3 showed the highest proliferation-inhibitory effect against MCF-7 cells with a cell viability of 56.39 ± 2.47% at the concentration of 500 μg/mL. While native PPs exhibited moderate anti-proliferation effect against MCF-7 cells at 500 μg/mL (34.71 ± 3.24%). Neither PPs nor LMP3 were comparable to the positive control relying on 5-FU. Galactoside containing molecules derived from pectin have been demonstrated to interact with a galectin 3-type lectin at the surface of proliferating mammalian cancer cells (Bushneva et al., 2002; Nangia-Makker et al., 2002), thus preventing tumor growth. Despite the similar structures and compositions between the native PPs and LMP3, their antitumor activity was distinct, suggesting the significance of molecular size in polysaccharide binding to galectin-3 of cancer cells (Sathisha, Jayaram, Nayaka, & Dharmesh, 2007). Moreover, the uptake of oligosaccharides by cancer cells was in a much better rate than that of intact PPs from the same sources, thus affecting the antitumor activity (Kapoor and Dharmesh, 2017).

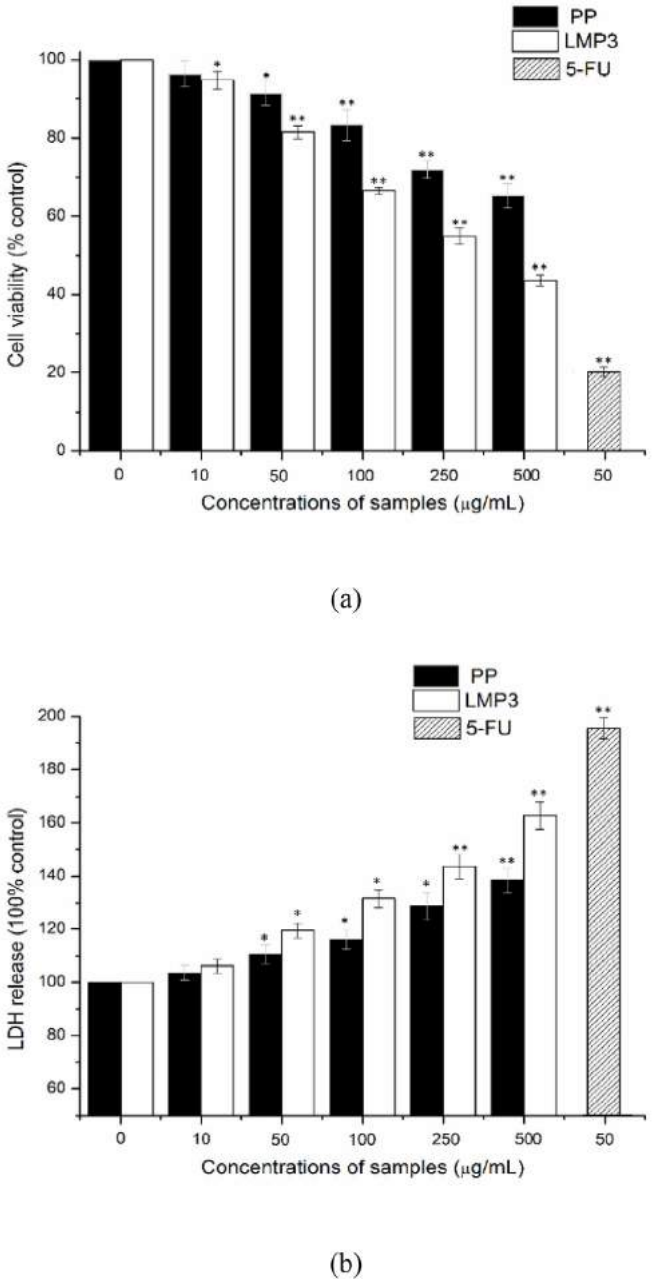

Fig. 8. (a) Effects of native PPs and LMP3 on the proliferation of MCF-7 cells. Cells were cultured in the presence of PPs and LMP3 (10–500 μg/mL) for 48 h and the cell growth was determined by the MTT assay. (b) Cytotoxic effects of native PPs and LMP3 on MCF-7 cells. Cells were cultured in the presence of PPs and LMP3 (10–500 μg/mL) for 48 h and 20 μL supernatant of the culture medium was used to assess LDH leakage into the media. Data are presented as mean ± S.D. (*) $P < 0.05$ and (**) $P < 0.01$ indicate statistically significant differences versus blank control groups.

LDH content is an indicator of loss in cell membrane integrity (G. X. Ma et al., 2014) and loss in membrane integrity occurs due to both necrosis and apoptosis death events (Murthy, Jayaprakasha, Kumar, Rathore, & Patil, 2011). The cytotoxicity of the two polysaccharides was evaluated to further confirm the proliferation inhibitory effect of native PPs and LMP3 on MCF-7 cells. LDH release of MCF-7 cells into the medium was significantly increased in a dose-dependent manner in the presence of the two polysaccharides ($P < 0.05$) (Fig. 8b). The content of LDH release triggered by LMP3 treatment at 500 μg/mL for 48 h was 162.8 ± 5.12% compared to the untreated cells, much higher than that of PPs (138.3 ± 2.5%). The results above indicated that LMP3 was endowed with higher cytotoxic effects against MCF-7 cells, which was consistent with cell viability assay.

4. Conclusion

In the present study, an effective ultrasound accelerated non-metal Fenton redox system relying on H_2O_2/ascorbic acid was established for the controlled depolymerization of PPs recycled from citrus canning processing water and the antitumor activity of resulting fragment was determined. Ultrasound can disaggregate PP clusters by mechanical effects and ultrasound/H_2O_2/ascorbic acid system generates a greater concentration of hydroxyl radical, depolymerizing PPs within minutes with these free radicals preferentially cleaving the GalA in the HG region. Thus, the HG region of PPs decreases throughout the depolymerization. Structural analysis demonstrates that ultrasound/H_2O_2/ascorbic acid depolymerization of PPs affords RG-I enriched LMPs with a highly branched structure of arabinan. The *in vitro* antitumor activities of native PPs and LMP3 were examined using MTT and LDH assay. The results suggest that LMP3 exhibited significantly higher antitumor activity against MCF-7 human breast cells compared to native PPs and that activity might be associated with their molecular size. These results suggest that the LMPs obtained from citrus canning processing water might be suitable for use in functional foods and potential therapeutic agents for human cancer. Thus, the free radical depolymerization of PPs may provide effective streams for either biological or industrial upgrading strategies aimed toward wastewater valorization.

Acknowledgements

This work was financially supported by the Key Research and Development Project of Zhejiang Province, China (2015C02036) and Public Welfare Project of Zhejiang Province, China (2015C32088).

Appendix A. Supplementary data

Supplementary data related to this article can be found at https://doi.org/10.1016/j.foodhyd.2018.05.025.

References

Arnous, A., & Meyer, A. S. (2009). Quantitative prediction of cell wall polysaccharide composition in grape (Vitis vinifera L.) and apple (Malus domestica) skins from acid hydrolysis monosaccharide profiles. *Journal of Agricultural and Food Chemistry, 57*(9), 3611–3619.

Bai, L., & Wang, J. (1998). Spin trapping - ESR study on the reaction of ascorbic acid with hydrogen peroxide. *Chemical Journal of Chinese Universities, 19*, 890–894.

Belén Gómez, B. G., Yáñez, R., Schols, H., & Alonso, J. L. (2016). Prebiotic potential of pectins and pectic oligosaccharides derived from lemon peel wastes and sugar beet pulp: A comparative evaluation. *Journal of Functional Foods, 20*, 108–121.

Bokare, A. D., & Choi, W. (2014). Review of iron-free Fenton-like systems for activating H_2O_2 in advanced oxidation processes. *Journal of Hazardous Materials, 275*, 121–135.

Bushneva, O. A., Ovodova, R. G., Shashkov, A. S., & Ovodov, Y. S. (2002). Structural studies on hairy region of pectic polysaccharide from campion Silene vulgaris (Oberna behen). *Carbohydrate Polymers, 49*(4), 471–478.

Carlotto, J., Souza, L. M., Baggio, C. H., Werner, M. F. D., Maria-Ferreira, D., Sassaki, G. L., et al. (2016). Polysaccharides from *Arctium lappa L.*: Chemical structure and biological activity. *International Journal of Biological Macromolecules, 91*, 954–960.

Chen, J. L., Cheng, H., Wu, D., Linhardt, R. J., Zhi, Z. J., Yan, L. F., et al. (2017). Green recovery of pectic polysaccharides from citrus canning processing water. *Journal of Cleaner Production, 144*, 459–469.

Chen, J., Liang, R. H., Liu, W., Li, T., Liu, C. M., Wu, S. S., et al. (2013). Pectic-oligosaccharides prepared by dynamic high-pressure nnicrofluidization and their in vitro fermentation properties. *Carbohydrate Polymers, 91*(1), 175–182.

Czechowska-Biskup, R., Rokita, B., Lotfy, S., Ulanski, P., & Rosiak, J. M. (2005). Degradation of chitosan and starch by 360-kHz ultrasound. *Carbohydrate Polymers, 60*(2), 175–184.

Dikeman, C. L., & Fahey, G. C. (2006). Viscosity as related to dietary fiber: A review. *Critical Reviews in Food Science and Nutrition, 46*, 649–663.

Dogan, M., Kayacier, A., & Ic, E. (2007). Rheological characteristics of some food hydrocolloids processed with gamma irradiation. *Food Hydrocolloids, 21*(3), 392–396.

Fellah, A., Anjukandi, P., Waterland, M. R., & Williams, M. A. K. (2009). Determining the degree of methylesterification of pectin by ATR/FT-IR: Methodology optimisation and comparison with theoretical calculations. *Carbohydrate Polymers, 78*, 847–853.

Garna, H., Mabon, N., Wathelet, B., & Paquot, M. (2004). New method for a two-step hydrolysis and chromatographic analysis of pectin neutral sugar chains. *Journal of Agricultural and Food Chemistry, 52*(15), 4652–4659.
Garrido-Ramirez, E. G., Theng, B. K. G., & Mora, M. L. (2010). Clays and oxide minerals as catalysts and nanocatalysts in Fenton-like reactions - a review. *Applied Clay Science, 47*(3–4), 182–192.
Gnanasambandam, R., & Proctor, A. (2000). Determination of pectin degree of esterification by diffuse reflectance Fourier transform infrared spectroscopy. *Food Chemistry, 68*, 327–332.
Gogate, P. R., & Prajapat, A. L. (2015). Depolymerization using sonochemical reactors: A critical review. *Ultrasonics Sonochemistry, 27*, 480–494.
Golash, N., & Gogate, P. R. (2012). Degradation of dichlorvos containing wastewaters using sonochemical reactors. *Ultrasonics Sonochemistry, 19*(5), 1051–1060.
Grohmann, K., Cameron, R. G., & Buslig, B. S. (1995). Fractionation and pretreatment of orange peel by dilute acid hydrolysis. *Bioresource Technology, 54*(2), 129–141.
Guo, X., Ye, X. Q., Sun, Y. J., Wu, D., Wu, N. A., Hu, Y. Q., et al. (2014). Ultrasound effects on the degradation kinetics, structure, and antioxidant activity of sea cucumber fucoidan. *Journal of Agricultural and Food Chemistry, 62*(5), 1088–1095.
Hao, M., Cheng, H. R., Xue, H. T., Zhang, T., Zhou, Y. F., & Tai, G. H. (2013). Comparative studies on the anti-tumor activities of high temperature- and pH-modifed citrus pectin. *Food Function, 4*, 960–971.
Joseph, C. G., Puma, G. L., Bono, A., & Krishnaiah, D. (2009). Sonophotocatalysis in advanced oxidation process: A short review. *Ultrasonics Sonochemistry, 16*(5), 583–589.
Kapoor, S., & Dharmesh, S. M. (2017). Pectic oligosaccharide from tomato exhibiting anticancer potential on a gastric cancer cell line: Structure-function relationship. *Carbohydrate Polymers, 160*, 52–61.
Karboune, S., & Khodaei, N. (2016). Structures, isolation and health-promoting properties of pectic polysaccharides from cell wall-rich food by-products: A source of functional ingredients. *Current Opinion in Food Science, 8*, 50–55.
Khalikov, D. K., & Mukhiddinov, Z. K. (2004). Physicochemical principles of plant-cell protopectin decomposition by aced catalysts. *Chemistry of Natural Compounds, 40*(2), 101–114.
Khodaei, N., & Karboune, S. (2016). Enzymatic generation of galactose-rich oligosaccharides/oligomers from potato rhamnogalacturonan I pectic polysaccharides. *Food Chemistry, 197*, 406–414.
Khotimchenko, M., Kovalev, V., Kolenchenko, E., & Khotimchenko, Y. (2012). Acidic method for the low molecular pectin preparation. *International Journal of Pharmacy and Pharmaceutical Sciences, 4*, 279–328 3.
Koda, S., Taguchi, K., & Futamura, K. (2011). Effects of frequency and a radical scavenger on ultrasonic degradation of water-soluble polymers. *Ultrasonics Sonochemistry, 18*(1), 276–281.
Leclere, L., Cutsem, P. V., & Michiels, C. (2013). Anti-cancer activities of pH- or heat-modifed pectin. *Frontiers in Pharmacology, 4*, 1–8.
Leonelli, C., & Mason, T. J. (2010). Microwave and ultrasonic processing: Now a realistic option for industry. *Chemical Engineering and Processing, 49*(9), 885–900.
Levigne, S., Ralet, M. C., & Thibault, J. F. (2002). Characterisation of pectins extracted from fresh sugar beet under different conditions using an experimental design. *Carbohydrate Polymers, 49*(2), 145–153.
Li, L. C., Li, J., & Gao, J. (2014). Functions of galectin-3 and its role in fibrotic diseases. *Journal of Pharmacology and Experimental Therapeutics, 351*(2), 336–343.
Li, J. H., Li, S., Zhi, Z. J., Yan, L. F., Ye, X. Q., Ding, T., et al. (2016). Depolymerization of fucosylated chondroitin sulfate with a modified Fenton-system and anticoagulant activity of the resulting fragments. *Marine Drugs, 14*(9), 1–13.
Marshall, W. L., & Franck, E. U. (1981). Ion product of water substance, O-degrees-C-1000-degrees-C, 1-10,000 bars - new international formulation and its background. *Journal of Physical and Chemical Reference Data, 10*(2), 295–304.
Matsumoto, T., Guo, Y. J., Ikejima, T., & Yamada, H. (2003). Induction of cell cycle regulatory proteins by murine B cell proliferating pectic polysaccharide from the roots of *Bupleurum falcatum L. Immunology Letters, 89*, 111–118.
Matsumoto, T., Moriya, M., Sakurai, M. H., Kiyohara, H., Tabuchi, H., & Yamada, H. (2008). Stimulatory effect of a pectic polysaccharide from a medicinal herb, the roots of *Bupleurum falcatum L.*, on G-CSF secretion from intestinal epithelial cells. *International Immunopharmacology, 8*, 581–588.
Ma, G. X., Yang, W. J., Mariga, A. M., Fang, Y., Ma, N., Pei, F., et al. (2014). Purification, characterization and antitumor activity of polysaccharides from Pleurotus eryngii residue. *Carbohydrate Polymers, 114*, 297–305.
Ma, X. B., Zhang, L. F., Wang, W. J., Zou, M. M., Ding, T., Ye, X. Q., et al. (2016). Synergistic Effect and mechanisms of combining ultrasound and pectinase on pectin hydrolysis. *Food and Bioprocess Technology, 9*(7), 1249–1257.
Miao, S. S., Mao, X. H., Pei, R., Miao, S. P., Xiang, C., Lv, Y. J., et al. (2013). Antitumor activity of polysaccharides from Lepista sordida against laryngocarcinoma in vitro and in vivo. *International Journal of Biological Macromolecules, 60*, 235–240.
Mokudai, T., Nakamura, K., Kanno, T., & Niwano, Y. (2012). Presence of hydrogen peroxide, a source of hydroxyl radicals, in acid electrolyzed water. *PLoS One, 7*(9), e46392.
Moreno, F. J., & Sanz, M. L. (2014). *Food oligosaccharides: Production, analysis and bioactivity*. New Jersey: Wiley-Blackwell (Chapter 1).
Murthy, K. N. C., Jayaprakasha, G. K., Kumar, V., Rathore, K. S., & Patil, B. S. (2011). Citrus limonin and its glucoside inhibit colon adenocarcinoma cell proliferation through apoptosis. *Journal of Agricultural and Food Chemistry, 59*(6), 2314–2323.
Nangia-Makker, P., Hogan, V., Honjo, Y., Baccarini, S., Tait, L., Bresalier, R., et al. (2002). Inhibition of human cancer cell growth and metastasis in nude mice by oral intake of modified citrus pectin. *Journal of the National Cancer Institute, 94*(24), 1854–1862.
Ramos-Aguilar, O. P., Ornelas-Paz, J. D., Ruiz-Cruz, S., Zamudio-Flores, P. B., Cervantes-Paz, B., Gardea-Bejar, A. A., et al. (2015). Effect of ripening and heat processing on the physicochemical and rheological properties of pepper pectins. *Carbohydrate Polymers, 115*, 112–121.
Sathisha, U. V., Jayaram, S., Nayaka, M. A. H., & Dharmesh, S. M. (2007). Inhibition of galectin-3 mediated cellular interactions by pectic polysaccharides from dietary sources. *Glycoconjugate Journal, 24*(8), 497–507.
Shin, K. S., Kiyohara, H., Matsumoto, T., & Yamada, H. (1997). Rhamnogalacturonan II from the leaves of Panax ginseng C.A. Meyer as a macrophage Fc receptor expression-enhancing polysaccharide. *Carbohydrate Research, 300*, 239–249.
Sun, Y. J., Ma, G. P., Ye, X. Q., Kakuda, Y., & Meng, R. F. (2010). Stability of all-trans-b-carotene under ultrasound treatment in a model system: Effects of different factors, kinetics and newly formed compounds. *Ultrasonics Sonochemistry, 17*, 654–661.
Uchiyama, H., Dobashi, Y., Ohkouchi, K., & Nagasawa, K. (1990). Chemical-change involved in the oxidative reductive depolymerization of hyaluronic-acid. *Journal of Biological Chemistry, 265*(14), 7753–7759.
Verma, P., Baldrian, P., & Nerud, F. (2003). Decolorization of structurally different synthetic dyes using cobalt(II)/ascorbic acid/hydrogen peroxide system. *Chemosphere, 50*(8), 975–979.
Wu, D., Cao, Y. M., Chen, J. C., Gao, H. F., Ye, X. Q., Liu, D. H., et al. (2016). Feasibility study on water reclamation from the sorting/grading operation in Mandarin orange canning production. *Journal of Cleaner Production, 113*, 224–230.
Wu, N., Ye, X. Q., Guo, X., Liao, N. B., Yin, X. Z., Hu, Y. Q., et al. (2013). Depolymerization of fucosylated chondroitin sulfate from sea cucumber, Pearsonothuria graeffei, via Co^{60} irradiation. *Carbohydrate Polymers, 93*(2), 604–614.
Yan, J. K., Pei, J. J., Ma, H. L., & Wang, Z. B. (2015). Effects of ultrasound on molecular properties, structure, chain conformation and degradation kinetics of carboxylic curdlan. *Carbohydrate Polymers, 121*, 64–70.
Yue, W., Yao, P. J., Wei, Y. N., Li, S. Q., Lai, F., & Liu, X. M. (2008). An innovative method for preparation of acid-free-water-soluble low-molecular-weight chitosan (AFWSLMWC). *Food Chemistry, 108*(3), 1082–1087.
Zhang, L. F., Ye, X. Q., Ding, T., Sun, X. Y., Xu, Y. T., & Liu, D. H. (2013a). Ultrasound effects on the degradation kinetics, structure and rheological properties of apple pectin. *Ultrasonics Sonochemistry, 20*(1), 222–231.
Zhang, L. F., Ye, X. Q., Xue, S. J., Zhang, X. Z., Liu, D. H., Meng, R. F., et al. (2013b). Effect of high-intensity ultrasound on the physicochemical properties and nanostructure of citrus pectin. *Journal of the Science of Food and Agriculture, 93*(8), 2028–2036.
Zhi, Z. J., Chen, J. L., Li, S., Wang, W. J., Huang, R., Liu, D. H., et al. (2017). Fast preparation of RG-I enriched ultra-low molecular weight pectin by an ultrasound accelerated Fenton process. *Scientific Reports, 7*, 1–11.